Int. J. Heat Mass Transfer. Vol. 34, No. 11, pp. 2925–2928, 1991
Printed in Great Britain

0017-9310/91 $3.00+0.00

Application of 'SPICE' to predict temperature distribution in heat pipes

H. M. Li, C. Y. Liu and M. Damodaran
School of Mechanical and Production Engineering, Nanyang Technological University, Nanyang Avenue, Singapore 2263

(*Received* 18 *January* 1991 *and in final form* 22 *March* 1991)

1. INTRODUCTION

The wall temperature difference between the evaporator and condenser portions of a heat pipe has been analysed by employing an analogous electrical circuit network [1–3]. In this conventional approach, the thermal resistance in the axial direction is usually negligible compared with that in the radial direction. Normally this condition can be satisfied if the heat pipe under consideration is long enough. According to this model, the outer wall temperature of the evaporator is maintained at T_e and that in the condenser at T_c. This causes a step discontinuity in temperature between the evaporator and condenser sections. For a given heat pipe with a fixed heat load, the temperature difference $T_e - T_c$ is a constant. However, the sharp discontinuity in temperature as defined by this conventional model does not exist in reality as confirmed by experimental results, for example ref. [4], which show a gradual variation in temperature between the evaporator and condenser section.

The object of this note is to present a new alternative approach to predict temperature distribution in heat pipes. In this method, temperature distribution in a heat pipe, modelled as an analogous electrical circuit, is predicted by applying SPICE [5], a general-purpose circuit simulation program developed by the researchers in the Department of Electrical Engineering and Computer Sciences at Berkeley, University of California. SPICE is used to simulate electrical circuit designs before the prototype is assembled. Useful predictions are obtained for heat pipes with and without adiabatic sections and for heat pipes with various evaporator and condenser lengths. Comparison of the predicted results with experiments demonstrates fairly good agreement. The note also shows how interdisciplinary developments could be used appropriately.

2. MODELLING

The heat transfer through the liquid-wick structure of the heat pipe is modelled as pure conduction by assuming an effective thermal conductivity. The thermal resistance of the vapour and the thermal resistance at the liquid/vapour interface are neglected. The vapour temperature is constant for a specified heat load and for the given dimensions of a heat pipe.

The heat pipe shown in Fig. 1(a), has three regions in the radial direction (i.e. wall, liquid-wick and vapour) and three different sections in the axial direction (i.e. evaporator, adiabatic section and condenser). The thermal performance of a heat pipe can be characterized by the network of thermal resistances, R_2 to R_8 and R_s; R_2, R_3 and R_4 represent the radial thermal resistance of the evaporator; R_6, R_7 and R_8 represent the radial thermal resistance of the condenser, while R_5 and R_s represent the axial resistance of the heat pipe. R_4, R_5 and R_6 are usually negligible compared with other resistances. R_s can be neglected provided $R_s/(R_2+R_3+R_7+R_8) > 20$ [3]. If each section of the heat pipe is divided into N_j elements (with subscript j = e, a, c denoting evaporator, adiabatic section and condenser respectively) in the axial direction, then by applying the overall network to each element, a new representative network, shown in Fig. 1(b), can be established. If the distribution of the heat load, Q, along the evaporator is uniform, the heat load through each element is given by

$$q_e = \frac{Q}{N_e}. \quad (1)$$

In each element, heat transfers in two paths, one in the radial path encountering the radial resistance, R', which is a series resistance comprising the radial pipe wall thermal resistance R_2 and the radial liquid-wick resistance R_3 and the other in axial path encountering the 'axial resistance', R'', which is a parallel resistance comprising the axial pipe wall resistance R_{s2} and the axial liquid-wick resistance R_{s3}. Hence

$$R' = R_2 + R_3 \quad (2a)$$

$$R'' = \frac{R_{s2} \cdot R_{s3}}{R_{s2} + R_{s3}} \quad (2b)$$

where

$$R_2 = \frac{\ln(d_o/d_i)}{2\pi k_p \Delta L_e} \quad (3a)$$

$$R_3 = \frac{\ln(d_i/d_v)}{2\pi k_e \Delta L_e} \quad (3b)$$

and

$$R_{s2} = \frac{\Delta L_e}{A_p k_p} \quad (4a)$$

$$R_{s3} = \frac{\Delta L_e}{A_w k_e} \quad (4b)$$

where ΔL_e is the length of each element which is related to the section length L_e and the corresponding number of elements N_e by

$$\Delta L_e = \frac{L_e}{N_e}. \quad (5)$$

The effective thermal conductivity of the liquid-wick region k_e is expressed as [2]

$$k_e = \frac{k_l[(k_l+k_w)-(1-\varepsilon)(k_l-k_w)]}{[(k_l+k_w)+(1-\varepsilon)(k_l-k_w)]} \quad (6)$$

where k_l and k_w are the heat conductivities of the liquid and the wick material, and ε is the porosity of the capillary wick.

Substituting equations (3), (4) and (5) into equation (2) gives

$$R' = R'_0 \cdot N_e \quad (7a)$$

$$R'' = R''_0 \cdot \frac{1}{N_e} \quad (7b)$$

where

$$R'_0 = \frac{\ln(d_o/d_i)}{2\pi k_p L_e} + \frac{\ln(d_i/d_v)}{2\pi k_e L_e} \quad (8a)$$

$$R''_0 = \frac{L_e}{A_p k_p + A_w k_e}. \quad (8b)$$

NOMENCLATURE

- A_p pipe cross-sectional area [m^2]
- A_w liquid-wick region cross-sectional area [m^2]
- d_o heat pipe outer diameter [m]
- d_i heat pipe inner diameter [m]
- d_v vapour core diameter [m]
- k_e effective heat conductivity of liquid-wick structure [$W\,m^{-1}\,{}^\circ C^{-1}$]
- k_p heat conductivity of the pipe wall material [$W\,m^{-1}\,{}^\circ C^{-1}$]
- L_a adiabatic section length [m]
- L_c condenser length [m]
- L_e evaporator length [m]
- N number of elements
- Q heat load of a heat pipe [W]
- q heat load of an element [W]
- R total thermal resistance of a heat pipe [${}^\circ C\,W^{-1}$]
- R_2, R_8 radial thermal resistance of the pipe wall [${}^\circ C\,W^{-1}$]
- R_3, R_7 radial thermal resistance of the liquid-wick region [${}^\circ C\,W^{-1}$]
- R_4, R_6 thermal resistance of the vapour/liquid interface [${}^\circ C\,W^{-1}$]
- R_5 axial thermal resistance of the vapour [${}^\circ C\,W^{-1}$]
- R_s axial thermal resistance of the pipe wall and the liquid-wick region [${}^\circ C\,W^{-1}$]
- R' radial thermal resistance of an element [${}^\circ C\,W^{-1}$]
- R'' axial thermal resistance of an element [${}^\circ C\,W^{-1}$]
- T_a wall temperature in the adiabatic section [${}^\circ C$]
- T_c wall temperature in the condenser [${}^\circ C$]
- T_e wall temperature in the evaporator [${}^\circ C$].

Greek symbol

- ε porosity of the capillary wick.

This shows that R' is directly proportional to the number of elements N_e, and R'' is inversely proportional to N_e. It can be shown that R'_0 and R''_0 are the radial thermal resistance and the axial thermal resistance when $N_e = 1$, equivalent to the overall radial resistance (R_2+R_3) and the overall axial resistance R_s respectively in the conventional model. As described above, normally $R''_0 \gg R'_0$ (magnitude of R''_0/R'_0 can be as large as 10^2 depending on the length of sections for a fixed radius of the pipe). Hence R''_0 is usually neglected as it is in parallel with R'_0. However, in the present model, if the number of elements N_e is large enough, it is possible to make the radial resistance R' and the axial resistance R'' compatible, thereby making it necessary to consider the axial thermal resistance.

The condenser can be modelled in a similar manner by substituting ΔL_e, L_e, N_e with ΔL_c, L_c, N_c respectively in equations (5), (7) and (8).

In the adiabatic section, there is no radial heat transfer since there is no temperature gradient in the radial direction. Hence $q_a = 0$ at every element. However, there is an axial temperature gradient. The thermal resistance can be derived from equations (7) and (8) by replacing ΔL_e, L_e, N_e with ΔL_a, L_a, N_a respectively.

The thermal network representation of the heat pipe is analogous to an electrical network, as thermal resistance, heat flux and temperature are analogous to electrical resistance, current and voltage. In order to determine the temperature values (or voltages) at every element (i.e. the wall temperature distribution), the circuit simulation software SPICE is employed in this study.

3. RESULTS AND DISCUSSION

Two heat pipes, A and B, are used to illustrate the application of SPICE to predict heat pipe wall temperature distribution. These are as follows:

Heat pipe A

This is copper walled, of circular cross-section with a wrapped screen wick made of 300-mesh stainless steel with 0.58 wick porosity and uses water as working fluid described in Phang [6]. The outer and inner diameters of the heat pipe are 0.0285 and 0.026 m, respectively.

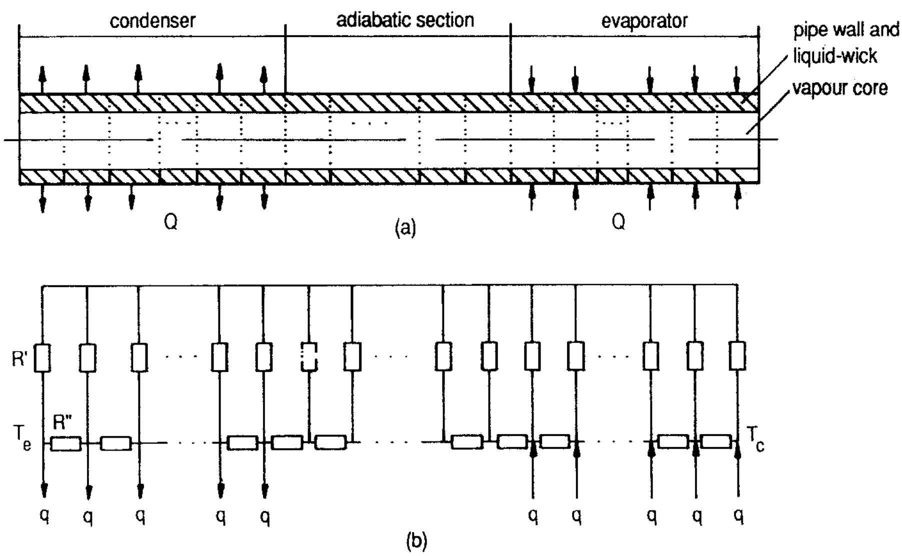

FIG. 1. Analogous circuit network of a heat pipe.

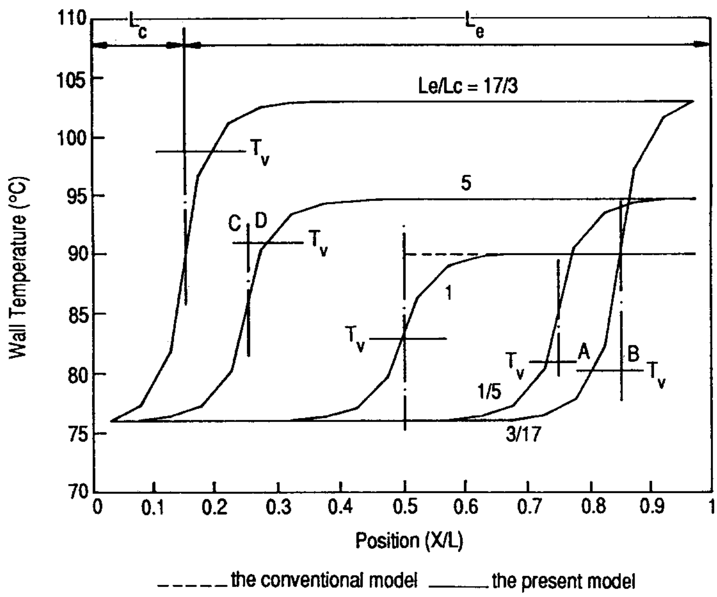

FIG. 2. Wall temperature profile of heat pipe without adiabatic section.

Heat pipe B

This is carbon steel walled, of circular cross-section with a 15-layer wrapped screen structure made of 100-mesh bronze wick material. The outer and inner diameters are 0.0337 and 0.0311 m. The 0.61 m long heat pipe has equal condenser and evaporator lengths and no adiabatic section. This is the one used by Huang and Tsuei [4] in their experimental measurements.

(*a*) *Heat pipe without adiabatic section and with equal evaporator and condenser length* $L_a = 0$, $L_e = L_c$

First the method is applied to heat pipe A to illustrate this case. The heat load Q is 300 W. The vapour core diameter is 0.0251 m and the condenser end wall temperature is 76°C. The values of K_p, K_w and K_l are 372, 17.3 and 0.668 W m^{-1} °C^{-1}. The value of R is 0.04667°C W^{-1}. The parameters such as q, R' and R'' are calculated using equations (1), (7) and (8) for all the elements. T_e or T_c can be specified depending on specific applications. In the present study, T_c was fixed. The calculated values are used in conjunction with SPICE, which will give the nodal temperature values as shown in Fig. 2. The wall temperature varies gradually between the evaporator and the condenser. In the regions near the two ends of the heat pipe the temperature varies very slowly and two platforms with T_e in the evaporator and T_c in the condenser can be seen from the curve for $L_e/L_c = 1$. Moreover, the relation between T_e and T_c follows the equation below, which is used in the conventional model:

$$\Delta T = T_e - T_c = QR \tag{9}$$

where R is the total thermal resistance. If R_4, R_5 and R_6 are neglected, R can be expressed as:

$$R = R_2 + R_3 + R_7 + R_8. \tag{10}$$

The vapour temperature is just the arithmetic mean of T_e and T_c [3]. The temperature of the vapour can also be obtained

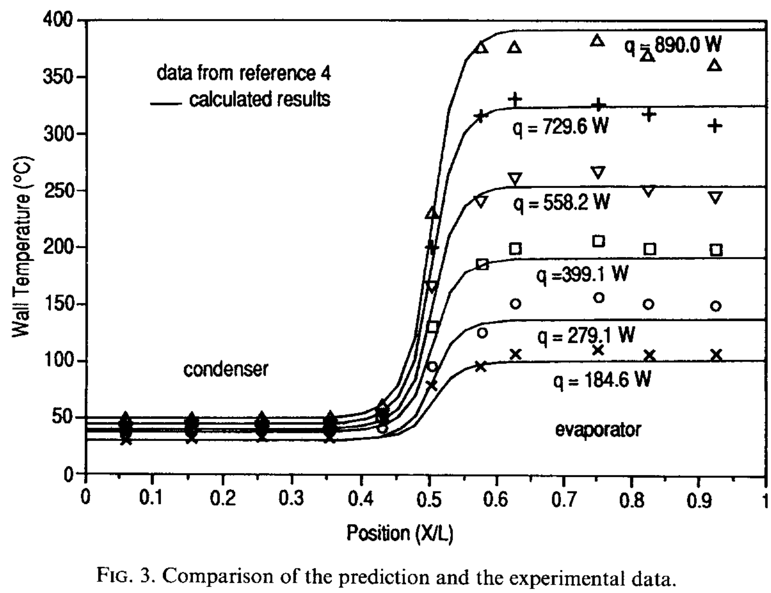

FIG. 3. Comparison of the prediction and the experimental data.

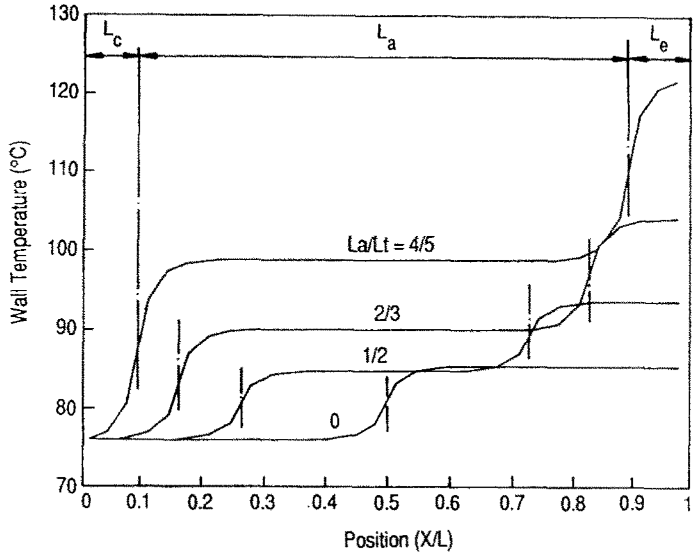

FIG. 4. Wall temperature profile of heat pipe with adiabatic section.

automatically from SPICE, since it is just a node's voltage in the network. The accuracy of the prediction is considered by varying the numbers of elements. Figure 2 also shows the comparison of two temperature profiles for $N = 20$ and 40, respectively. As the difference between the two curves is negligible, the temperature profile can be considered to be adequately represented by using $N = 20$.

The method is next applied to predict the outer wall temperature of the heat pipe B for total heat load ranging from 184.6 to 890.0 W.

Figure 3 compares the predicted results with the experimental measurements of Huang and Tsuei [4]. It can be seen that a fairly good agreement has been achieved by the prediction based on an average conductance of 0.296 W °C^{-1} for the heat pipe.

(b) Heat pipes with three distinct sections and with equal lengths of evaporators and condensers, $L_a \geqslant 0$, $L_e = L_c$

Heat pipe A is used to illustrate this case. In this case the heat input q_a at the nodes in adiabatic section is zero. From the prediction it can be seen that $T_v = T_a = (T_e + T_c)/2$. This is because there is no radial temperature gradient in adiabatic section. Figure 4 shows the predicted axial temperature distribution for a constant heat load Q, condenser end wall temperature T_c and the total L_t. The curves show that as the adiabatic length increases, the evaporator wall temperature T_e increases, as does the vapour temperature. When L_a increases to some values, for example, $L_a/L_t = 4/5$, the temperature platforms in the evaporator and in the condenser, as shown in the other three curves, do not exist.

(c) Heat pipes without adiabatic sections and with various lengths of evaporators and condensers, $L_a = 0$, $L_e < L_c$ *or* $L_e > L_c$

Heat pipe A is used to illustrate this case. Figure 2 shows the predicted temperature distribution for different combinations of L_e and L_c for constant Q, T_c and L_t. The results show that as L_e increases, the vapour temperature increases and vice versa. From the temperature distribution for a fixed ratio L_e/L_c and that for the corresponding inverse ratio L_c/L_e, it can be seen that the temperature difference $\Delta T = T_e - T_c$ is the same. It can be shown that when $L_e/L_c = 1$, ΔT is a minimum and the thermal resistance is also a minimum. Figure 2 also shows that if $L_e/L_c > 1$, e.g. $L_e/L_c = 5$, the wall temperature in the region C–D is lower than the vapour temperature, implying that the vapour will condense in that part of the evaporator that it is not supposed to and thereby making the effective condensation length longer than the physical condenser length. Similarly, when $L_e/L_c < 1$, e.g. $L_e/L_c = 3/17$, the wall temperature in the region A–B is higher than the vapour temperature, so the vapour cannot condense in that part of the condenser as it is supposed to, thereby making the effective condensation length shorter than the physical condenser length. When $L_e/L_c = 1$, the evaporator and the condenser can perform fully as the evaporating section and the condensing section, respectively.

4. CONCLUSION

The application of the software package SPICE to predict the wall temperature distribution along a heat pipe has been demonstrated. The predictions show fairly good agreement with the existing experimental data. This method is useful in addressing cases when the heat flux distribution along the pipe is non-uniform or when there are multiple heat sources or heat sinks located along the pipe. SPICE is able to solve these kind of problems easily and quickly, as the parameters at each node are supplied independently. This also highlights how computer developments in other disciplines of study can be used appropriately.

REFERENCES

1. P. Dunn and D. A. Reay, *Heat Pipes*. Pergamon Press, London (1982).
2. S. W. Chi, *Heat Pipe Theory and Practice*. Hemisphere, Washington, DC (1976).
3. ESDU Data Item No. 79012, Heat pipes—performance of capillary-driven designs, Engineering Sciences Data Unit, London (1979).
4. B. J. Huang and J. T. Tsuei, A method of analysis for heat pipe exchangers, *Int. J. Heat Mass Transfer* **28,** 553–562 (1985).
5. P. W. Tuinenga, *SPICE: A Guide to Circuit Simulation and Analysis Using PSpice*. Prentice-Hall, New York (1988).
6. C. M. Phang, Heat pipes: design, construction and testing, Final Year Project Report, School of Mechanical and Production Engineering, Nanyang Technological Institute, Singapore (1988).